

Supporting Information

**Synthesis of Borasiloxanes by Oxidative Hydrolysis of Silanes and Pinacolborane using
 $\text{Cu}_3(\text{BTC})_2$ as Solid Catalyst**

Aamarajothi Dhakshinamoorthy^{*a}, Abdullah M. Asiri,^b Patricia Concepcion,^c Hermenegildo Garcia^{*b,c}

^aSchool of Chemistry, Madurai Kamaraj University, Tamil Nadu, India 625 021.

^bCentre of Excellence for Advanced Materials Research, King Abdulaziz University, Jeddah, Saudi Arabia.

^cInstituto Universitario de Tecnología Química CSIV-UPV, Universitat Politècnica de València, Av. De los Naranjos s/n, 46022, Valencia, Spain.

Experimental section

Materials

$\text{Cu}_3(\text{BTC})_2$ commercially known as Basolite C 300 MOF was supplied by BASF. Dimethylphenyl silane, diphenylsilane, triphenylsilane and phenylsilane used in the present study was purchased from Sigma Aldrich and used as received. Solvents and other reagents like HBpin, B_2pin were received from Sigma.

Instrumentation

Powder XRD diffraction patterns were measured in the reflection mode in a Philips X'Pert diffractometer using the $\text{CuK}\alpha$ radiation ($\lambda = 1.54178 \text{ \AA}$) as the incident beam, PW3050/60 (2 theta) as Goniometer, PW 1774 spinner as sample stage, PW 3011 as detector, incident mask fixed with 10 mm. PW3123/10 for Cu was used as a monochromator. PW3373/00 Cu LFF was used as X-ray tube with power scanning of 45 kV and 40 mA current. The sample powder was loaded into a holder and levelled with a glass slide before mounting it on the sample chamber. The specimens were scanned between 2° and 70° with the scan rate of $0.02^\circ/\text{s}$.

X-ray photoelectron spectra were collected using a SPECS spectrometer equipped with a 150-MCD-9 detector and using a non monochromatic $\text{MgK}\alpha$ (1253.6 eV) X-Ray source. Spectra were recorded using analyzer pass energy of 50 eV, an X-ray power of 50 W and under an operating pressure of 10^{-9} mbar. During data processing of the XPS spectra, binding energy (BE) values were referenced to C1s peak (284.5 eV). Spectra treatment has been performed using the CASA software.

IR spectra of adsorbed NO were recorded at low temperature (-165°C) with a Nexus 8700 FTIR spectrophotometer using a DTGS detector and acquiring at 4 cm^{-1} resolution. An

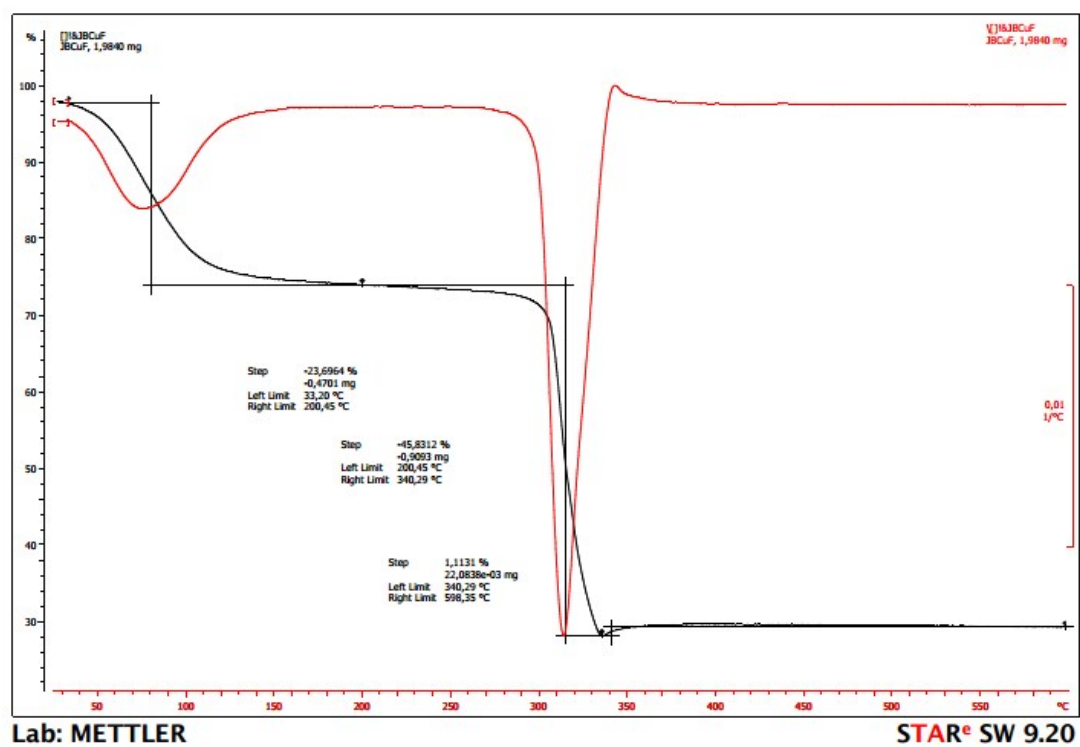
IR cell allowing in situ treatments in controlled atmospheres and temperatures from -176 °C to 500 °C was connected to a vacuum system with gas dosing facility. For IR studies the samples were pressed into self-supported wafers and pre-treated in vacuum (10^{-4} mbar) at 150 °C for 1h. After activation the samples were cooled down to -165 °C under dynamic vacuum conditions followed by NO dosing at increasing pressure (0- 0.4mbar). IR spectra were recorded after each dosage.

For the in situ studies, after sample pre-treatment, 2.8 mbar silane was adsorbed at 25° C followed by evacuation and co-adsorption of 2.8 mbar borane. Afterwards the sample was evacuated, in order to remove physisorbed species, and the temperature increased to 50 °C and then to 70°C. The sample was kept 1h at each temperature.

Reaction procedure

In a typical reaction, 30 mg of $\text{Cu}_3(\text{BTC})_2$ was added to 2 mL of acetonitrile containing 0.5 mmol of dimethylphenylsilane and 0.5 mmol of HBpin, keeping the reaction mixture under nitrogen atmosphere. Then, this reaction mixture was introduced in a preheated oil bath at the required temperature and submitted to magnetic stirring for the required time as indicated in Table 1. It was observed that the reaction mixture turns from blue to pale green with the evolution of hydrogen gas. The reaction progress was monitored by gas chromatography and after completion of the reaction, the mixture was washed twice with acetonitrile and filtered. Then, the product is analyzed by gas chromatography for its purity and quantification. Conversion and selectivity were determined by Agilent gas chromatography using internal standard method. The same procedure is followed for the reusability experiments. Formation of these type of products has been already reported.¹

Figure S1. TGA of $\text{Cu}_3(\text{BTC})_2$



XPS Studies

In order to analyze the nature of copper species in the $\text{Cu}_3(\text{BTC})_2$ MOF sample, XPS and FT-IR studies of NO as probe molecule were performed. The $\text{Cu}_{2p_{3/2}}$ core level XPS line shown in Figure S3 exhibits a main component at 934.6 eV and an intense shake-up structure at 944.04 eV and 939.7 eV. While the presence of the satellite peak is characteristic of Cu^{2+} species,² the $\text{Cu}_{2p_{3/2}}$ XPS BE (934.6 eV), the Cu LMN Auger line (915.76 eV) and the Cu α Auger parameter (1850.4 eV), are anomalous compared to Cu^{2+} species. Similar behavior has been also observed in copper containing zeolites and attributed to relaxation energies due to the presence of isolated dispersed copper ions (Cu^{2+} and Cu^+) inside the zeolite matrix.^{3,4} Due to this behavior, quantitative analysis of the $\text{Cu}^+/\text{Cu}^{2+}$ ratio is difficult to assess from the XPS data.

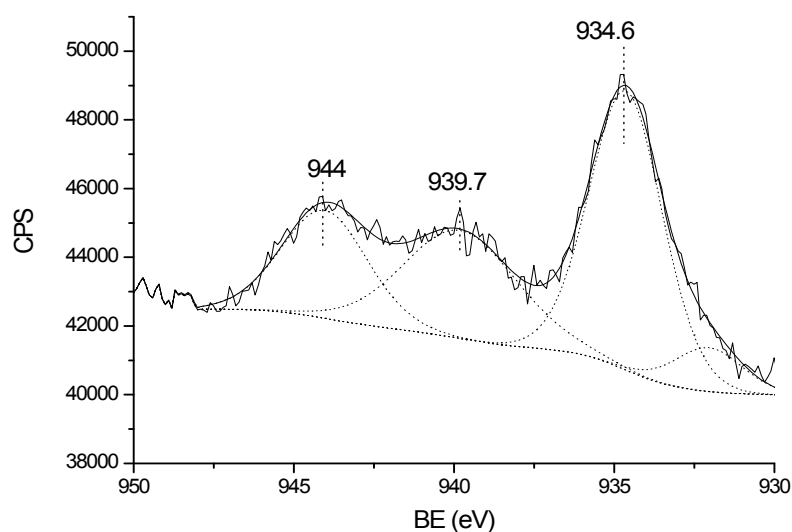


Fig.S2 $\text{Cu}_{2p_{3/2}}$ XPS line of $\text{Cu}_3(\text{BTC})_2$.

FT-IR using NO as probe molecule

Taken into account the high sensitivity of NO as an IR probe molecule for identification of Cu^+ and Cu^{2+} species,⁵ IR studies have been performed at $-165\text{ }^\circ\text{C}$ using NO as a probe molecule. The IR spectra shown in Figure S4 shows two bands at 1890 cm^{-1} and 1742 cm^{-1} , growing in intensity at increasing NO loading, and a small shoulder at 1951 cm^{-1} . The IR band at 1890 cm^{-1} can be associated to $(\text{Cu}^{2+}\text{-OH})$ species⁶ or to hydroxy groups of the MOF structure,⁷ the small shoulder at 1951 cm^{-1} to Cu^{2+} species⁸ and the IR band at 1742 cm^{-1} to Cu^+ mononitrosyl species.⁹ Thus, from a qualitative point of view different copper species, as $\text{Cu}^{2+}\text{-OH}$, Cu^{2+} and Cu^+ can clearly been detected in the $\text{Cu}_3(\text{BTC})_2$ MOF while quantization of those species is not possible.

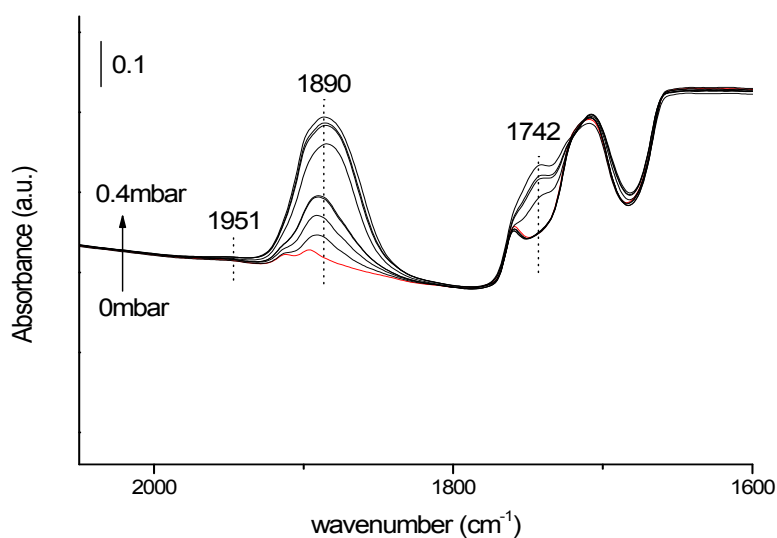


Fig.S3. IR spectra of NO adsorption at $-165\text{ }^\circ\text{C}$ on $\text{Cu}_3(\text{BTC})_2$ MOF sample. Spectra measured at increasing NO dosing (0-0.4mbar).

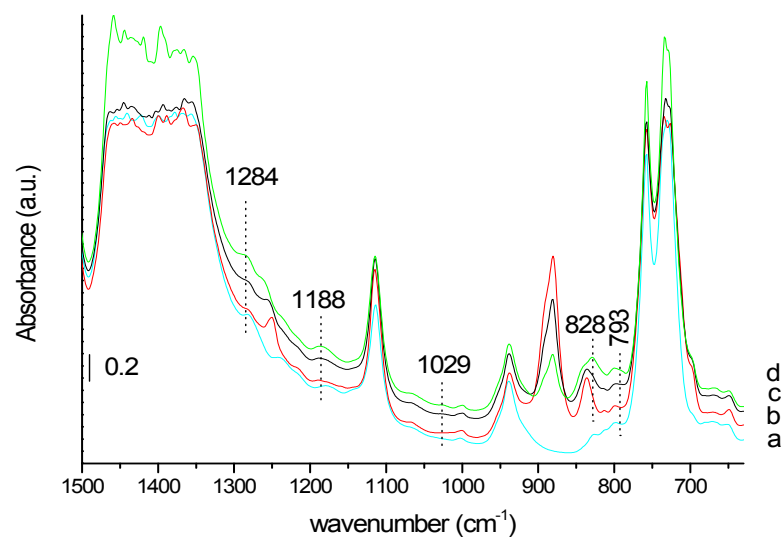


Fig.S4 IR spectra of fresh $\text{Cu}_3(\text{BTC})_2$ (a), and after 2.8 mbar **1** adsorbed at 25 °C (b), followed by increasing temperature to 50 °C (c) and 70 °C (d).

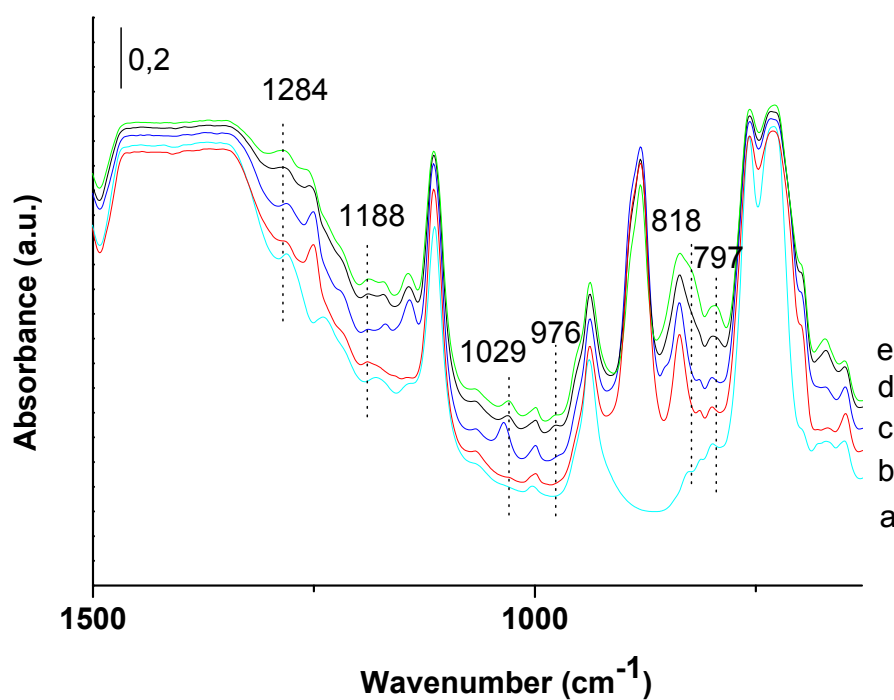
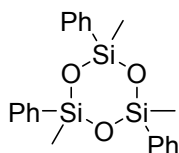


Figure S5. IR spectra of pre-reacted $\text{Cu}_3(\text{BTC})_2$ sample (a), after 2.8 mbar **1** adsorbed at 25 °C (b), 2.6 mbar HBpin co-adsorbed at 25 °C (c), and followed by increasing temperature to 50 °C (d) and at 70 °C (e).



Scheme S1. Structure of 2,4,6-trimethyl-2,4,6-triphenyl-1,3,5,2,4,6-trioxatrisilinane.

Hot filtration test

The heterogeneous nature of the process was confirmed by performing a hot filtration test in which the temporal profile of the conversion of **1** is compared in two twin experiments. In one of the cases, the reaction is carried out in the presence of catalyst, while in the other the solid catalyst is removed by hot filtration after 1 h and the clear solution in the absence of any solid is allowed to react further under the reaction conditions. The results obtained are also presented in Figure 1. As it can be seen there, the reaction stops almost completely upon filtration of the catalyst when the conversion of **1** was about 28 %, observing in the absence of catalyst only around 8% increment in the conversion after 4 h.

Heterogeneity and reuse experiments

The heterogeneous nature of the process was confirmed by performing a hot filtration test as explained above. In addition, ICP analysis showed that less than 2 ppm of copper leached to the solution. The catalyst stability was further assessed by reusing $\text{Cu}_3(\text{BTC})_2$ in two consecutive reuses. It was observed that the conversion of **1** to be 100, 59 and 39% for fresh, first and second reuses. This decrease in activity is associated to the appearance of new peaks at low angle in the powder XRD patterns of the two times used $\text{Cu}_3(\text{BTC})_2$ catalyst (Fig. S6). However, in spite of the appearance of new peaks, it seems that the crystallinity of $\text{Cu}_3(\text{BTC})_2$ is retained during the reuse experiments.

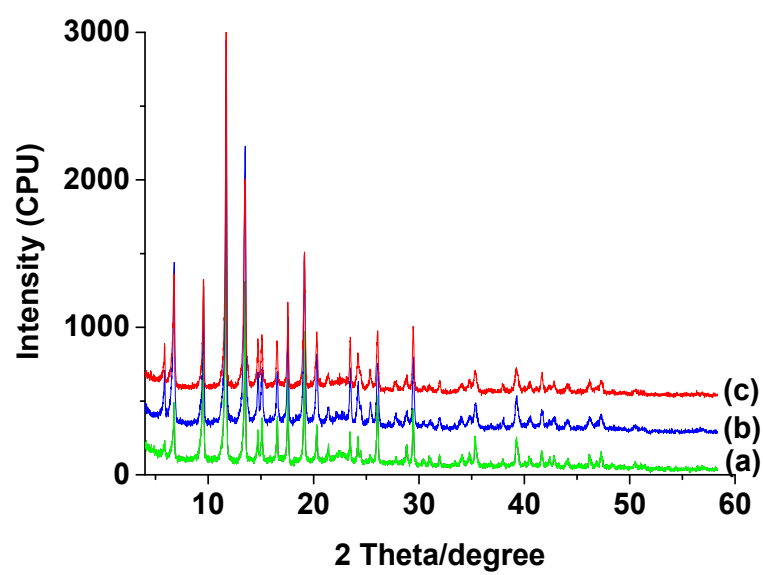


Fig. S6. Powder XRD patterns of fresh (a), recovered (b) and two times reused $\text{Cu}_3(\text{BTC})_2$ (c) catalysts.

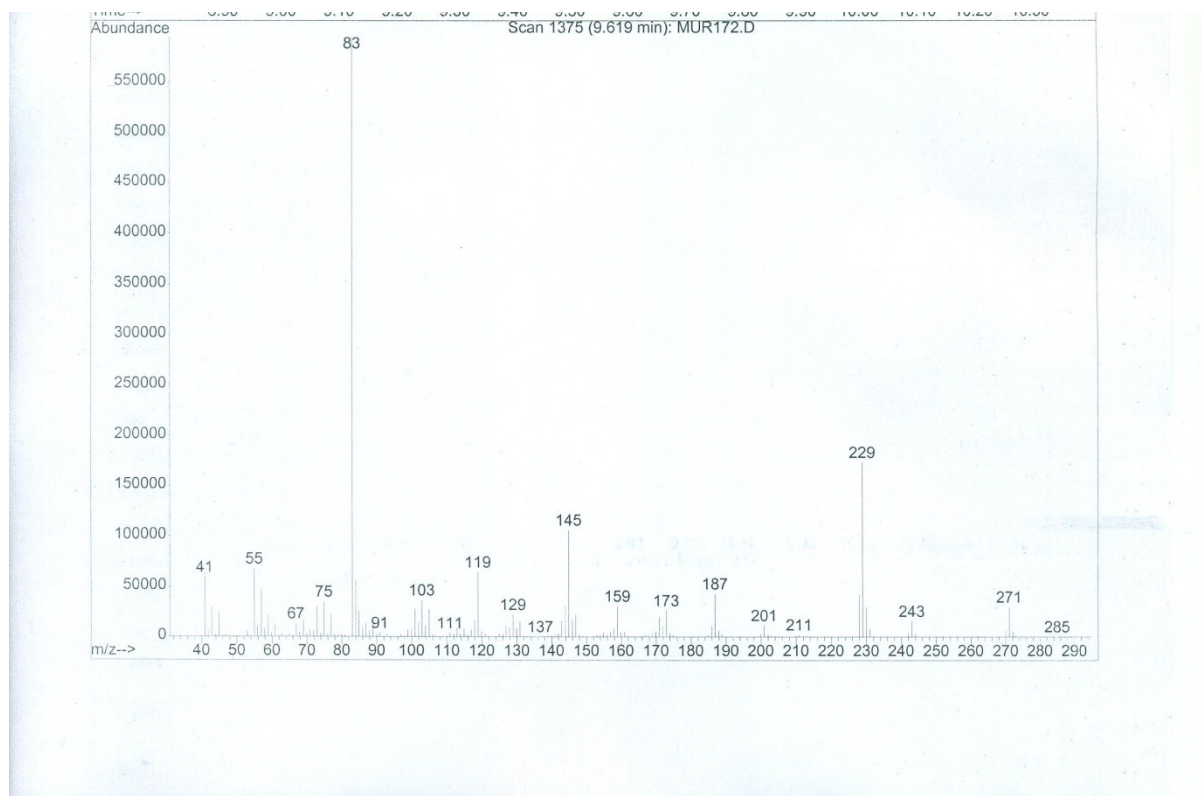


Fig. S7. GC-MS spectrum of di-t-butylborosiloxane. m/z 229 corresponds to the removal of t-butyl group from the m/z value of 286.

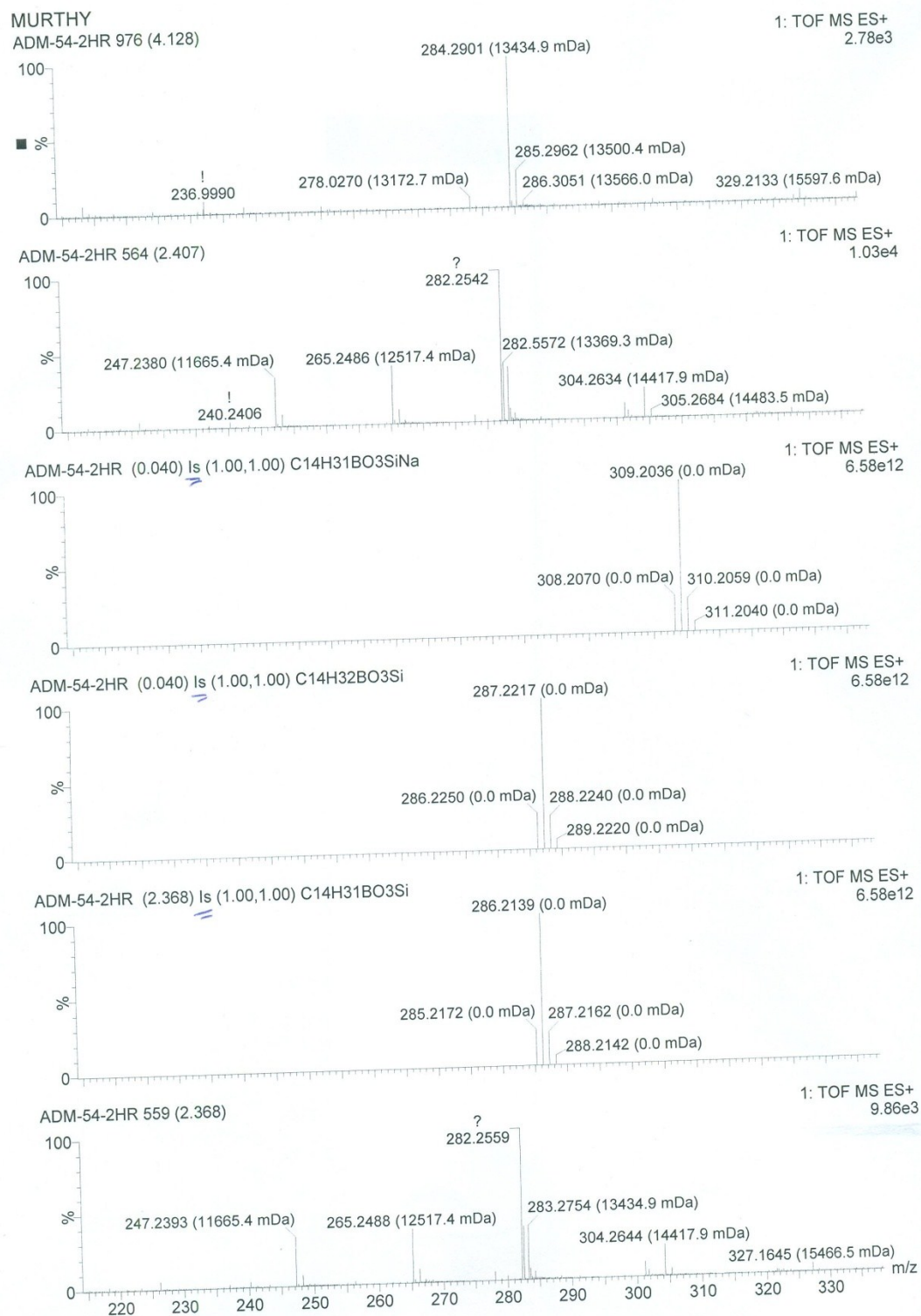


Fig. S8. HR-MS spectrum of di-*t*-butylborosiloxane. The HR-MS value of this compound is given as $M+H$ and $M+Na$

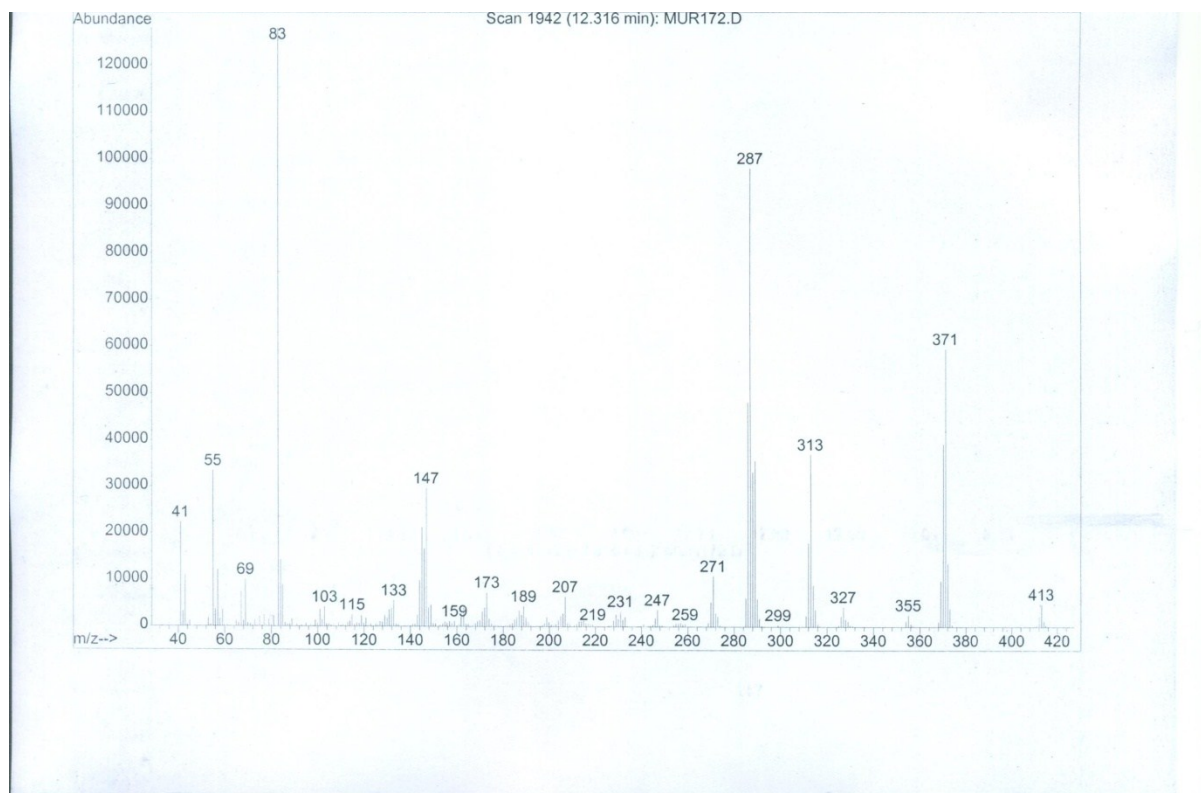


Fig. S9. GC-MS spectrum of di-*t*-butyldiborosiloxane (dimer product). m/z 371 corresponds to the removal of *t*-butyl group from the m/z value of 428.

Elemental Composition Report

Page 1

Single Mass Analysis

Tolerance = 5.0 PPM / DBE: min = -1.5, max = 50.0

Element prediction: Off

Number of isotope peaks used for i-FIT = 3

Monoisotopic Mass, Even Electron Ions

483 formula(e) evaluated with 1 results within limits (up to 50 closest results for each mass)

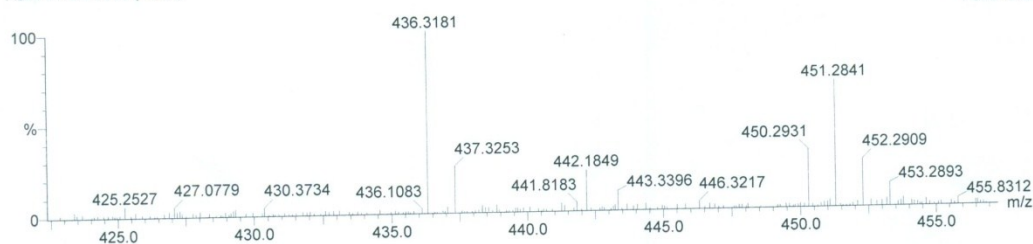
Elements Used:

C: 0-21 H: 0-43 B: 0-2 O: 0-6 Na: 0-1 Si: 0-3 K: 0-1

MURTHY

ADM-54-2HR 967 (4.095)

1: TOF MS ES+
1.97e+002



Minimum:				-1.5					
Maximum:		5.0	5.0	50.0					
Mass	Calc. Mass	mDa	PPM	DBE	i-FIT	i-FIT (Norm)	Formula		
451.2841	451.2834	0.7	1.6	1.5	62.9	0.0	C20	H42	B2 O6
							Na	Si	

Fig. S10. HR-MS spectrum of di-t-butylidiborosiloxane (dimer product). The HR-MS value of this compound is given as M+Na.

References

1. C. Kleeberg, M. S. Cheung, Z. Lin and T. B. Marder, *J. Am. Chem. Soc.*, 2011, **133**, 19060-19063.
2. B.R. Strohmeier, D.E. Leyden, R.S. Field, D.M. Hercules, *J. Catal.*, 1985, 94, 514-530.
3. W. Grünert, N.W. Hayes, R.W. Joyner, E.S. Shpiro, M. Rafiq H. Siddiqui and G.N. Baeva, *J. Phys. Chem.* 1994, 98, 10832-10846.
4. A. Corma, A. Palomares, F. Marquez, *J. Catal.*, 1997, 170, 132-139.
5. nG.T. Palomino, S. Bordiga, A. Zecchina, G.L. Marra, C. Lamberti, *J. Phys.Chem. B.*, 2000, 104, 8641-8651.

6. F. Giordanino, P. N. R. Vennestrom, L. F. Lundegaard, F. N. Stappen, S. Mossin, P. Beato, S. Bordiga, C. Lamberti, Dalton Trans. 2013, 12741-12761.
7. P. Concepcion, M. Boronat, R. Millán, M. Moliner, A. Corma, Catal. Today 2017, in press.
8. R. Kefirov, A. Penkova , K. Hadjiivanov, S. Dzwigaj, M. Che, Microporous and Mesoporous Materials 116 (2008) 180.
9. T. Venkov, K. Hadjiivanov, A. Milushev, D. Klissurski, Langmuir 2003, 19, 3323-3332.